BioGecko
Vol 12 Issue 03 2023
ISSN NO: 2230-5807

TO INVESTIGATE BEHAVIOR OF PILES IN SOIL WITH VARIOUS SOIL CONDITIONS

Mr. Pravin U Sabde[1], Prof. Dr. Manish Patkar[2]
[1]Department of Civil Engineering, Oriental University, Indore
[2]Associate Professor, Department of Civil Engineering, Oriental University, Indore

Abstract: Wave activity generates lateral strains on pile groups that support coastal and offshore structures. These lateral stresses have cyclic amplitudes and durations. The mechanics of lateral overloaded pile behavior are more complex than the mechanics of axial compressive piles. A better understanding of pile-soil interactions under laterally cyclic stresses is required to provide more effective design solutions for these types of foundations. Pile spacing has a significant impact on the maximum settlements, final settlements, and load bearing capabilities of piles after geological and geotechnical tests. Total deformation, shear stress, and corresponding stress are studied in connection to various soil conditions and soil types. In the first step, all Is 11841 code requirements for NDCT design are examined, and a finite element analysis in ANSYS is given against identity and applied loads against various dimensions. Total deformation, strain energy, and shear stress graphs for thickness. The total deformation graph shows the results for diameters 1300mm - 150.78mm, 1400mm - 160.78m, and 1500mm - 162.72m. Thickness 300mm is 0.0328, thickness 400mm is 0.0124, and thickness 500mm is 0.0150. There is presently a scarcity of knowledge on how to apply a performance-based paradigm to pile performance, particularly in liquefiable soil.

Keywords: Pile foundation, soil, ANSYS, Pile cyclic loading

1. Introduction:

1.1 General:

Wave activity creates lateral stresses on the pile groups sustaining coastal and offshore constructions. These lateral stresses have varying amplitudes and durations and are cyclic in nature. The mechanics of a group of laterally laden piles behave in a more complicated way than a group of axially loaded piles. Due to pile-soil-pile interaction, the lateral load capacity of the pile group is lowered when surrounding piles that are similarly loaded have an effect on the piles in the group that are subjected to lateral loading. Under cyclic lateral loading, pile group behavior is nonlinear and involves complex group interaction. Clay deposits are used to build the majority of pile foundations in maritime areas. Cyclical loading in clay under undrained conditions causes stiffness to deteriorate and shear strength to decrease. Higher deflections and higher bending moments than static loading are caused by issues related to cyclic lateral loading in clay, including gap formation at the pile-soil interface, buildup of excess pore pressure, and remolding of the clay. In many different areas of civil engineering, such as with offshore and onshore wind turbines or with structures for transportation infrastructure, cyclical loading of pile foundations is crucial. Offshore wind turbines and waves may provide cyclic loads, as can temperature-induced restrictions (integral bridges without joints and bearings). Under cyclic loading, soils of all grain sizes exhibit complex behaviors. For instance, cyclic lateral stresses on sand piles cause the soil to either become looser or denser around the piles. However, adjustments to the more straightforward monotonic loading criteria are still often used in the construction of pile foundations under cyclic stress. To develop more effective design solutions for these kinds of foundations, it is consequently necessary to have a better knowledge of the interaction between piles and soil under lateral cyclic loads. Centrifuge model tests on single piles and freestanding pile groups in dry silica sand have been conducted at the Centre for Offshore Foundation Systems (COFS) in Perth, Australia, as part of a research project to create a framework for quantifying cyclic effects on piles.

The lateral displacement of sloping land caused by flow liquefaction has caused many pile foundations to fail, especially those in ports and harbor structures. Numerous research have identified and shown that by simulating liquefied soils as viscous fluids, the behavior of these materials may be precisely predicted. Numerous methods can be used to estimate the effects of lateral soil movements on piles, including I empirical methods, II methods based on the subgrade reaction model, III methods utilizing the linear elastic theory, IV limit equilibrium analysis, V viscous flow theory, and VI numerical analysis using the finite element method.

Pile foundation seismic design in liquefiable soils poses extremely difficult analytical and design challenges. The pile foundation may experience severe shaking even when the ground is entirely liquefied and the soil stiffness is at its lowest. During this shaking, the pile is vulnerable to significant cracking or even breakage. Additionally, relative to the non-liquefied situation, liquefaction may cause a significant increase in pile cap displacements. After liquefaction, there may be significant lateral spreading or down slope displacements depending on whether the soil's residual strength is greater than the static shear stresses brought on by a sloping site or a free surface like a river bank. Moving soil might subject the piles to damaging pressures that could cause them to collapse. The Niigata earthquake in 1964 and the Kobe earthquake in 1995 both saw a lot of failures of this sort.

When a non-liquefied layer is pulled along by the advancing liquefied earth, lateral spreading is most devastating. The profession has only recently begun to properly address these significant design challenges. The improvement is the outcome of analytical developments and findings from shaking table and centrifuge tests. These developments have made it possible for case study reviews to be more thorough and fundamental, and they have increased awareness of design issues.

Piled foundations are often selected as a foundation choice in possibly liquefiable soil owing to their shown ability to perform effectively in prior earthquakes where soil liquefied as a result of seismic stresses. However, there are documented instances of piles losing support as a result of failing to withstand the increased stresses caused by liquefied earth. Designing geotechnical structures in accordance with their performance is prioritized by the Performance-Based Earthquake Engineering (PBEE) concept (ISO-23469, 2005). This calls for the evaluation and design of structures whose seismic performance satisfies the needs of modern society. Performance-based design acknowledges the need to determine the deformation requirements for a given earthquake level because seismic loading is an imposed deformation. Therefore, deformation constraints for both global and local component levels may be used to compare applied deformation to. Information on how to use a performance-based paradigm to improve pile performance, particularly in liquefiable soil, is currently lacking.

Objective:

- ❖ The objective of the study is to perform time history analysis for group of pile for different size and shape pile cap during liquefaction on pile group.

2. Literature Review:

2.1 Introduction:

The lateral reaction of pile groups has been studied in the past using full-scale experiments, centrifuge model tests, 1-g model tests, and numerical calculations. This chapter discusses the need for additional research, the limitations of the current research, and a review of earlier studies.

2.2 Research Performed by Various Authors:

Abdel-Salam Ahmed Mokhta et. Al., 2014 examines the one of the main causes of bridge collapses during earthquakes is believed to be the instability of the piles caused by the liquefaction of loose sand. In this work, the seismic behavior of piles penetrated into liquefiable sandy soil is examined using the 3D finite element program DIANA 9.3. A specific Line-Solid Connection element is added to this model to represent the contact between the pile and the surrounding soil. The effects of soil submergence, pile diameter, earthquake magnitude, and duration on pile lateral deformation and produced bending moment along pile shaft were the subject of extensive experiments. According to study results, quake size and duration have a distinct impact on the generation of pore water pressure, which in turn affects pile lateral deformation and bending moments. They also emphasize the benefits of managing lateral displacement with relatively large piles. Designers are advised to do thorough research and guard against plastic hinge and buckling failures. Shivanand Mali et. Al., 2018 conducted study on Typically, piled-raft foundations are used to support offshore structures. Using three-dimensional finite element modeling, a massive heaped raft was numerically simulated in this work. This study sought to ascertain how raft-soil stiffness ratio, pile spacing, pile length, and pile diameter affected the settlement, load distribution, bending moments, and shear force behavior of a substantial piled-raft foundation. The results showed that both the average and differential settlement ratios effectively decreased and then gradually increased as pile separation increased up to 5 to 6 times the diameter of the pile. It was discovered that rafts with lower raft-to-soil stiffness ratios and higher pile group-to-raft width ratios performed better at reducing the average settlement ratio. As pile separation increased, the load-sharing ratio decreased, but it increased as pile length did. Up until the pile group to raft width ratio reached 0.6, the bending moment ratio increased as pile spacing increased and decreased as pile length increased.

Sandro Carbonari et. Al., 2017 examines the effects of soil-structure interaction brought on by various pile group geometries and pile inclinations, this study examines the seismic response of bridge piers supported on inclined pile groups in a variety of soil deposits. Using a direct method and a numerical model they developed for the analysis of inclined pile groups, the authors perform frequency domain studies. The soil is conceptualized as a visco-elastic medium made up of infinitely thin, independent horizontal layers, in contrast to the beam elements used to describe the superstructure and piles. Elastodynamic Green's functions, which include hysteretic and radiation damping, are used to simulate the interactions between soil and piles as well as pile-pile-soil interactions in the frequency domain. Kinematic interaction analyses are used to investigate the importance of kinematic stress results in piles, the foundation filtering effect, and the rotational component of the input motion due to the coupled roto-translational behavior of the soil-foundation system. These investigations uncovered crucial data for understanding the fundamental mechanisms underlying the system of soil, foundation, and structure's dynamic response. The outcomes of numerical simulations show that the typical design methodologies advised by codes do not accurately predict the displacements and stress consequences of superstructures. Elarabi et. Al., A technical document from 2014 explains the micropile's brief history, classification, drilling methods, grouting, reinforcement, design idea, testing procedures, and micropile guidelines. The study offers a simplified, sequential design process. These include techniques for Micropiles testing, extra structural concerns, service limit states, and geotechnical strength limit states. Zhiguo Zhang et. Al., 2018 conducted study on the majority of current design practices for calculating the mechanics of tunnel-soil-pile interactions are based on Winkler's foundation, which has significant drawbacks like ignoring the continuity of the soil foundation. The effects of lateral soil displacements on pile behavior are not taken into account in the analytical studies that are currently in use, which heavily rely on plane strain evaluations. The analytical technique should consider a number of characteristics, such as ground shearing displacements and the impact of lateral soil displacements next to the pile, in order to increase the accuracy of the forecast of pile behavior caused by tunneling. In order to predict the lateral displacements and internal forces of a single-pile and group-piles produced by tunneling while taking into account the effects of lateral soil displacements, a simplified solution based on Pasternak's foundation model is presented in this article. First, using Pasternak's foundation model, a simplified solution for the tunnel-soil-pile interaction is developed. The impact of foundation shearing displacements is illustrated by this solution. Second, to take into consideration the effect of lateral soils adjacent to the pile, the pile is supplied with equal focused forces across the shear layer. The validity of the solutions is confirmed by the results of the boundary element program, the centrifuge test data, and the field measurements. The calculated results are also contrasted with those obtained with and without taking tunnel-soil-pile interaction into account. The results are shown to be more in line with the data from the centrifuge test as well as the observed in-situ displacements when the effects of lateral soil displacements are taken into consideration. Additionally, the shear layer modulus, pile diameter, ground-loss ratio, pile-tunnel distance, and pile spacing are investigated as factors affecting single-pile and group-pile displacements. Because it is impossible to ignore the impact of soil shear displacements on pile reaction, using Winkler's foundation model to solve this problem could lead to mistakes.

3. Methodology:

Fig 1: Flowchart

3.1 Introduction:

To meet the study goals, a series of stationary and non - stationary base shear testing on 2 single piling and four pile groupings were performed at the experimental site listed below

(a) Site Assessment,
(b) Cycling Lateral Loading Testing of Singles Pile team in ANSYS
(c) ANSYS Cyclic Lateral Load Assessment of Four Pile Group
(d) ANSYS Dynamic Lateral Loading Assessment of 2 Free Pile Group Cyclic Lateral Pressure Assessment of such a Resolved Pile Collective inside ANSYS
(e) Validation using Sites Observation Data.

3.2 Problem Statement from Site Data:

- Diameter of pile = 1300mm,
- No of piles = 8
- Depth of pile cap =1500mm
- Dead weight of pier, pier cap and pile cap
- With 15% buoyancy =16250 KN
- With 100% buoyancy= 11200KN
- Dead weight of girder and footpath =1337.3KN
- Live load (two span loaded) = 3719.5KN
- (One span loaded) = 2052.7 KN
- Frictional force due to DL = 40 KN
- Moment = 949.5 KN
- Longitudinal force (for two span loaded) =688.8KN
- Moment= 688.8*23.677KNm
- For one span loaded=728.92KN
- Moment=728.92*23.677KNm

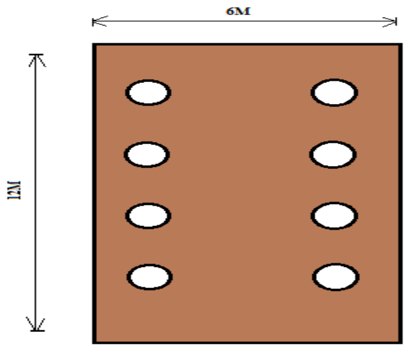

Fig 2: Pile Foundations

1. **Taking Diameter as Variable W.R.T. Constant Length**

DIAMETER mm		
1300	**1400**	**1500**

2. **Taking Thickness of Pile Cap as Variable**

THICKNESS mm		
300	400	500

4. RESULTS AND DISCUSSION

4.1. Results for different diameters

- **Total Deformation**

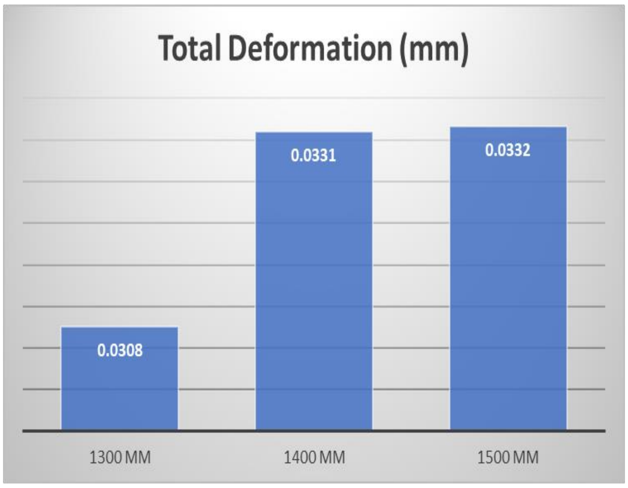

Graph. 1 Total Deformation for diameter

Above graph describes the result total deformation, total deformation for diameter 1300mm is 0.0308, for diameter 1400 is 0.0331 and for diameter 1500 is 0.0332. As per diameter the result is in increasing order.

- **Normal Stress**

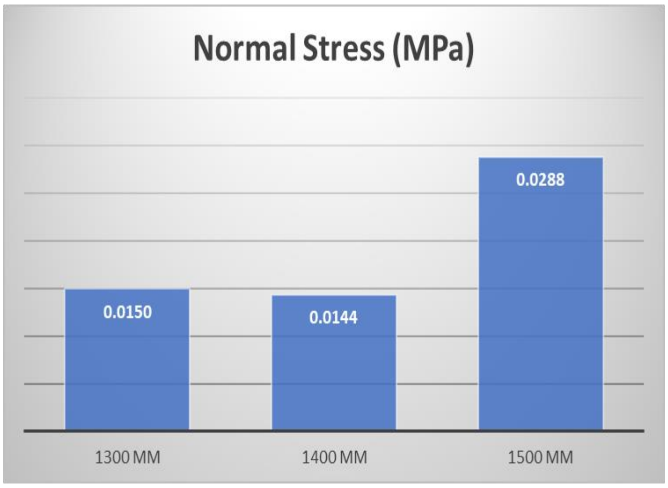

Graph.2 Normal stress for diameter

Above graph describes the result Normal stress, Normal stress for diameter 1300mm is 0.0150, for diameter 1400 is 0.0144 and for diameter 1500 is 0.0288. As per diameter the result is in increasing order.

- **Shear Stress**

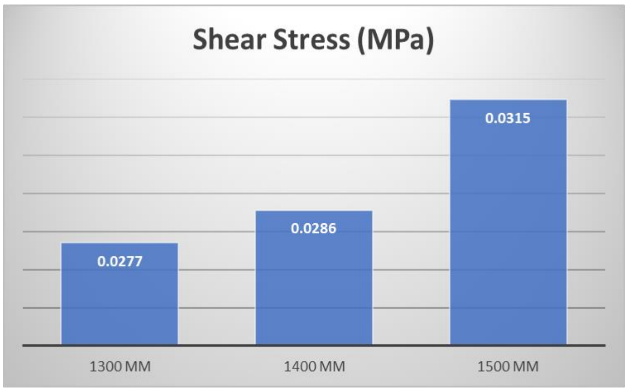

Graph.3 Shear stress for diameter

Above graph describes the result Shear stress, Shear stress for diameter 1300mm is 0.0277, for diameter 1400 is 0.0286 and for diameter 1500 is 0.0315. As per diameter the result is in increasing order.

- **Strain Energy**

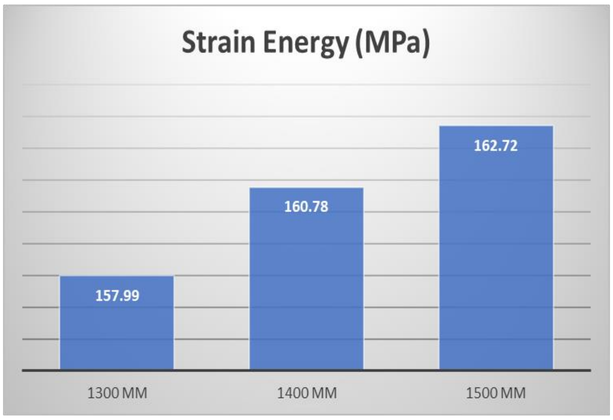

Graph 4 Strain Energy for diameter

Above graph describes the result Strain Energy, Strain Energy for diameter 1300mm is 157.99, for diameter 1400 is 160.78 and for diameter 1500 is 162.72. As per diameter the result is in increasing order.

4.2 ANSYS modeling of case study:

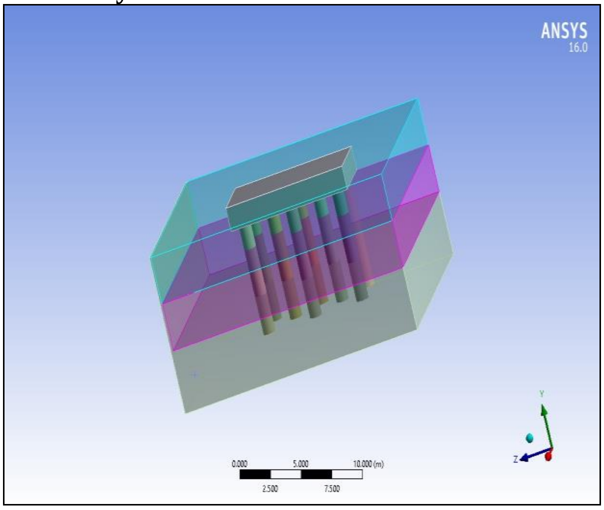

Fig 5: Modelling

The above figure shows modelling of pile foundation in software ANSYS.

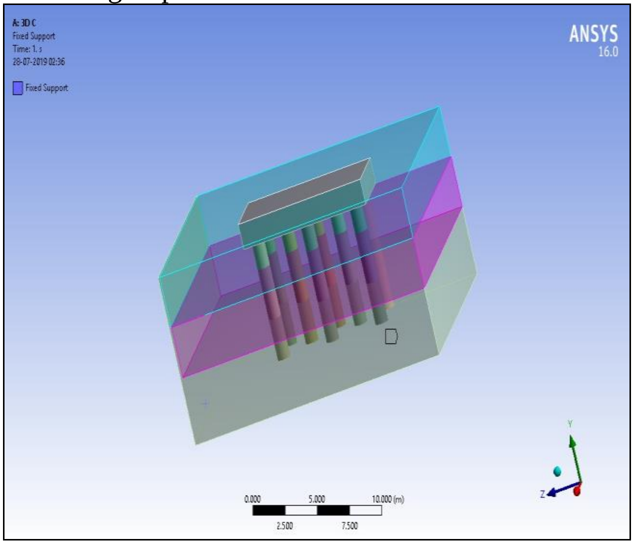

Fig 6: Fixed Support

4.3 Different Thickness of pile cap

1. Thickness 300mm

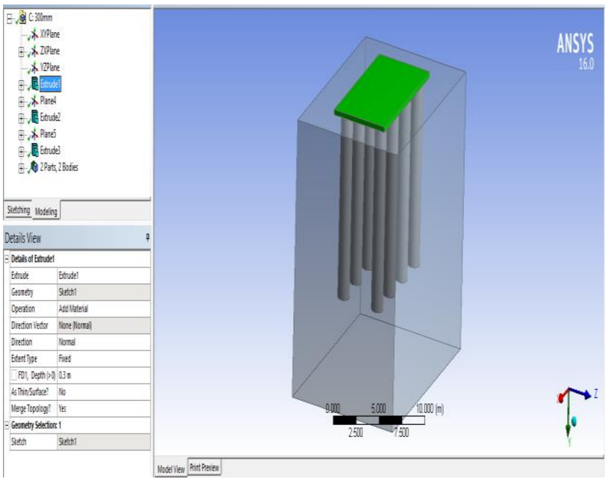

Details View

Details of Extrude1	
Extrude	Extrude1
Geometry	Sketch1
Operation	Add Material
Direction Vector	None (Normal)
Direction	Normal
Extent Type	Fixed
☐ FD1, Depth (>0)	0.3 m
As Thin/Surface?	No
Merge Topology?	Yes
Geometry Selection: 1	
Sketch	Sketch1

Fig 7: Model Geometry for Thickness 300mm

Above figure shows model geometry for thickness 300 in software ANSYS.

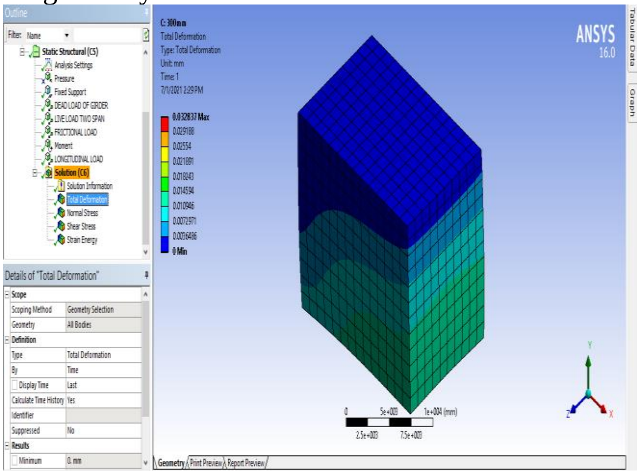

C: 300mm
Total Deformation
Type: Total Deformation
Unit: mm
Time: 1
7/1/2021 2:29 PM

Details of "Total Deformation"

Scope	
Scoping Method	Geometry Selection
Geometry	All Bodies
Definition	
Type	Total Deformation
By	Time
☐ Display Time	Last
Calculate Time History	Yes
Identifier	
Suppressed	No
Results	
☐ Minimum	0. mm

Fig 8: Total Deformation for

4.4 Thickness 300mm

Above figure shows total deformation for thickness 300 in software ANSYS.

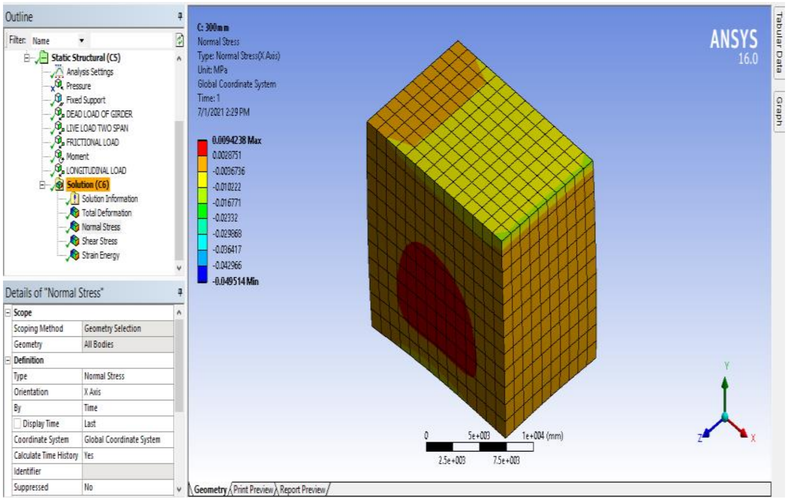

C: 300mm
Normal Stress
Type: Normal Stress(X Axis)
Unit: MPa
Global Coordinate System
Time: 1
7/1/2021 2:29 PM

Details of "Normal Stress"

Scope	
Scoping Method	Geometry Selection
Geometry	All Bodies
Definition	
Type	Normal Stress
Orientation	X Axis
By	Time
☐ Display Time	Last
Coordinate System	Global Coordinate System
Calculate Time History	Yes
Identifier	
Suppressed	No

Fig 9: Normal Stress for Thickness 300mm

Above figure shows normal stress for thickness 300 in software ANSYS.

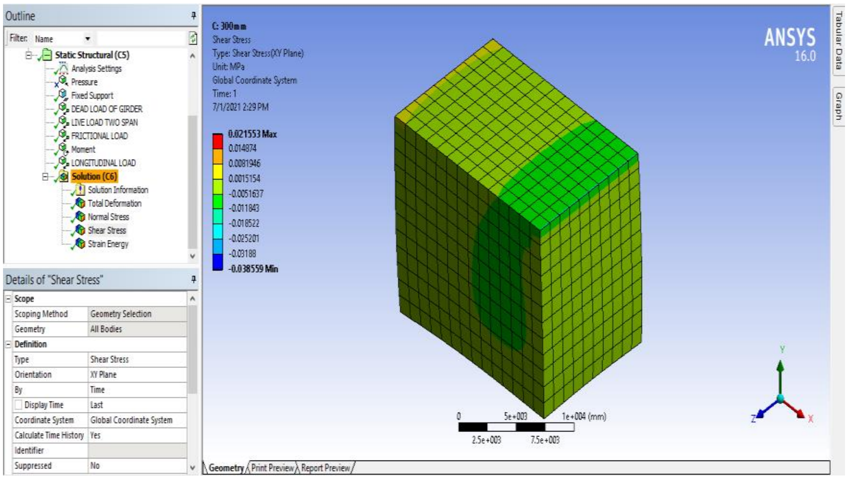

C: 300mm
Shear Stress
Type: Shear Stress(XY Plane)
Unit: MPa
Global Coordinate System
Time: 1
7/1/2021 2:29 PM

Details of "Shear Stress"

Scope	
Scoping Method	Geometry Selection
Geometry	All Bodies
Definition	
Type	Shear Stress
Orientation	XY Plane
By	Time
☐ Display Time	Last
Coordinate System	Global Coordinate System
Calculate Time History	Yes
Identifier	
Suppressed	No

Fig 10: Shear stress for Thickness 300mm

Above figure shows shear stress for thickness 300 in software ANSYS.

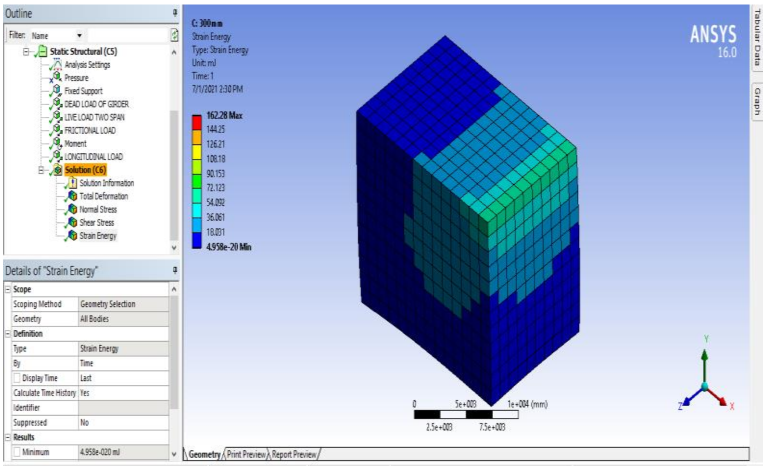

C: 300mm
Strain Energy
Type: Strain Energy
Unit: mJ
Time: 1
7/1/2021 2:30 PM

Details of "Strain Energy"

Scope	
Scoping Method	Geometry Selection
Geometry	All Bodies
Definition	
Type	Strain Energy
By	Time
☐ Display Time	Last
Calculate Time History	Yes
Identifier	
Suppressed	No
Results	
☐ Minimum	4.958e-020 mJ

Fig 11: Strain Energy for Thickness 300mm

Above figure shows strain energy for thickness 300 in software ANSYS.

4.5 Thickness 400mm

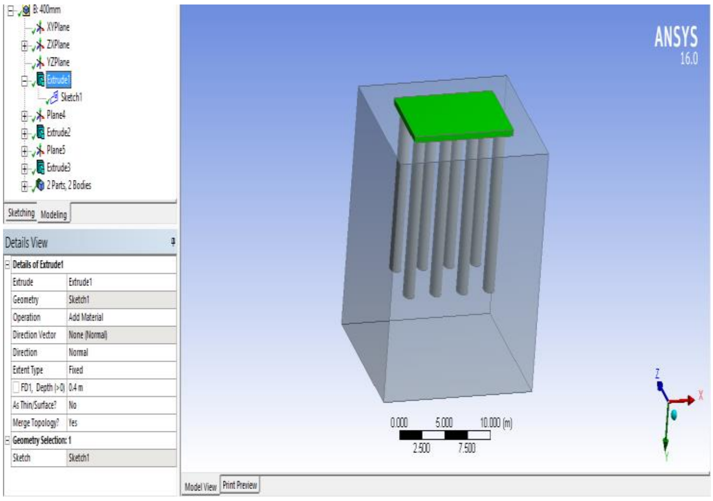

Details View

Details of Extrude1	
Extrude	Extrude1
Geometry	Sketch1
Operation	Add Material
Direction Vector	None (Normal)
Direction	Normal
Extent Type	Fixed
☐ FD1, Depth (>0)	0.4 m
As Thin/Surface?	No
Merge Topology?	Yes
Geometry Selection: 1	
Sketch	Sketch1

Fig 12: Model Geometry for Thickness 400mm

Above figure shows model geometry for thickness 400 in software ANSYS.

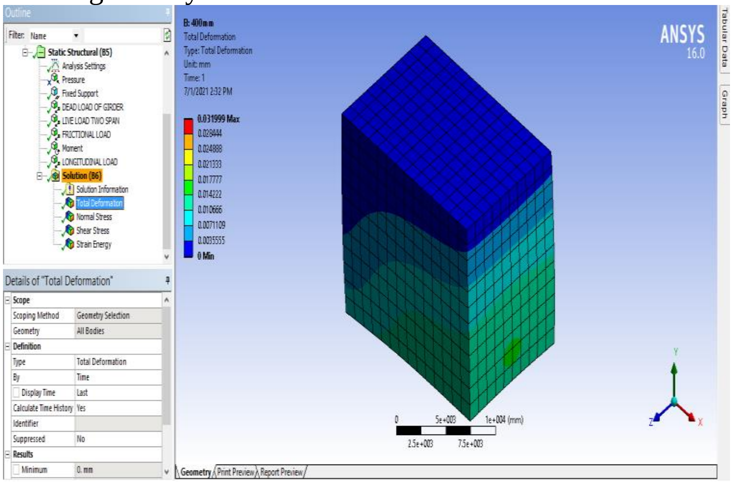

B: 400mm
Total Deformation
Type: Total Deformation
Unit: mm
Time: 1
7/1/2021 2:32 PM

Details of "Total Deformation"

Scope	
Scoping Method	Geometry Selection
Geometry	All Bodies
Definition	
Type	Total Deformation
By	Time
☐ Display Time	Last
Calculate Time History	Yes
Identifier	
Suppressed	No
Results	
☐ Minimum	0. mm

Fig 13: Total Deformation for Thickness 400mm

Above figure shows Total Deformation for thickness 400 in software ANSYS.

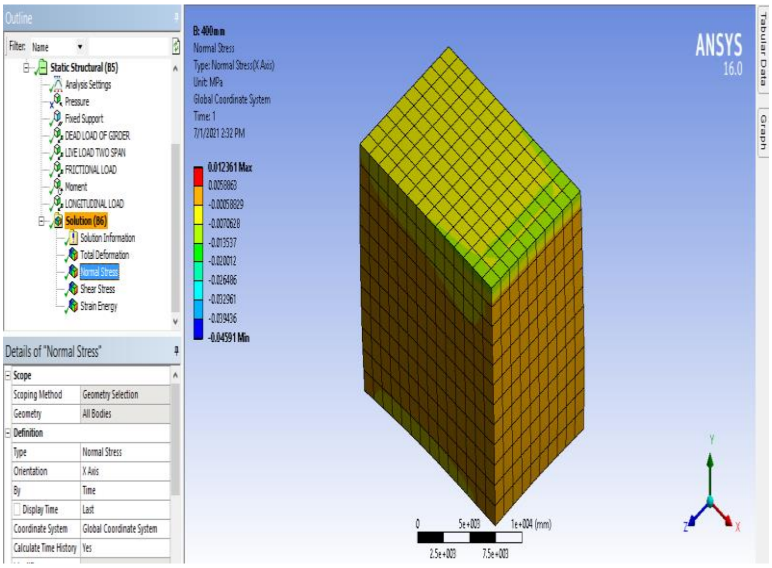

B: 400mm
Normal Stress
Type: Normal Stress(X Axis)
Unit: MPa
Global Coordinate System
Time: 1
7/1/2021 2:32 PM

Details of "Normal Stress"

Scope	
Scoping Method	Geometry Selection
Geometry	All Bodies
Definition	
Type	Normal Stress
Orientation	X Axis
By	Time
☐ Display Time	Last
Coordinate System	Global Coordinate System
Calculate Time History	Yes

Fig 14: Normal Stress for Thickness 400mm

Above figure shows Normal Stress for thickness 400 in software ANSYS.

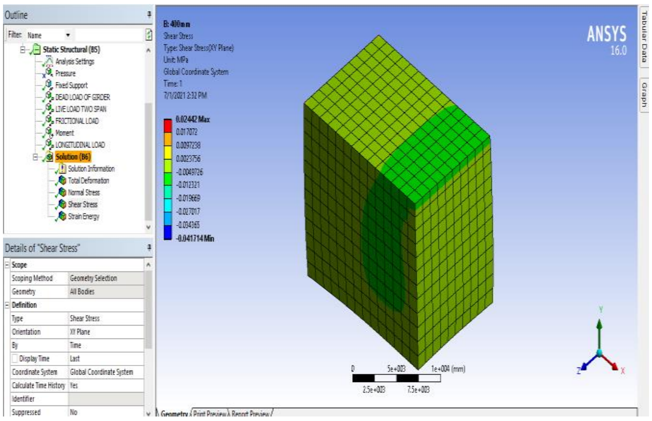

B: 400mm
Shear Stress
Type: Shear Stress(XY Plane)
Unit: MPa
Global Coordinate System
Time: 1
7/1/2021 2:32 PM

Details of "Shear Stress"

Scope	
Scoping Method	Geometry Selection
Geometry	All Bodies
Definition	
Type	Shear Stress
Orientation	XY Plane
By	Time
☐ Display Time	Last
Coordinate System	Global Coordinate System
Calculate Time History	Yes
Identifier	
Suppressed	No

Fig 15: Shear Stress for Thickness 400mm

Above figure shows Shear Stress for thickness 400 in software ANSYS.

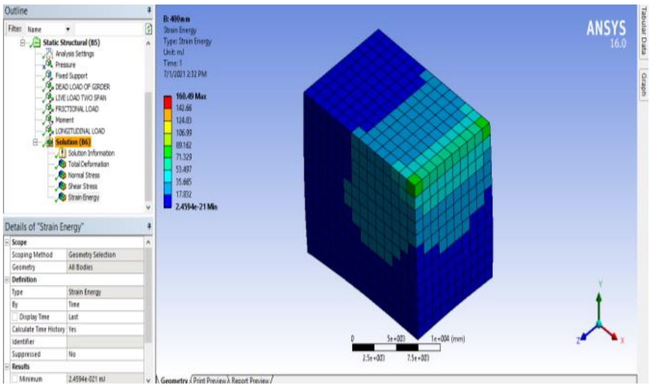

B: 400mm
Strain Energy
Type: Strain Energy
Unit: mJ
Time: 1
7/1/2021 2:32 PM

160.49 Max
142.66
124.83
106.99
89.162
71.329
53.497
35.665
17.832
2.4594e-21 Min

Details of "Strain Energy"

Scope	
Scoping Method	Geometry Selection
Geometry	All Bodies
Definition	
Type	Strain Energy
By	Time
☐ Display Time	Last
Calculate Time History	Yes
Identifier	
Suppressed	No
Results	
☐ Minimum	2.4594e-021 mJ

Fig 16: Strain Energy for Thickness 400mm

Above figure shows Strain Energy for thickness 400 in software ANSYS.

4.6 Thickness 500mm

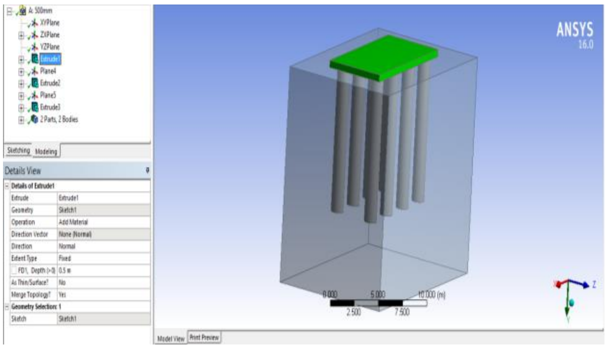

Details View

Details of Extrude1	
Extrude	Extrude1
Geometry	Sketch1
Operation	Add Material
Direction Vector	None (Normal)
Direction	Normal
Extent Type	Fixed
☐ FD1, Depth (>0)	0.5 m
As Thin/Surface?	No
Merge Topology?	Yes
Geometry Selection: 1	
Sketch	Sketch1

Fig 17: Model Geometry for Thickness 500mm

Above figure shows Model Geometry for thickness 500 mm in software ANSYS.

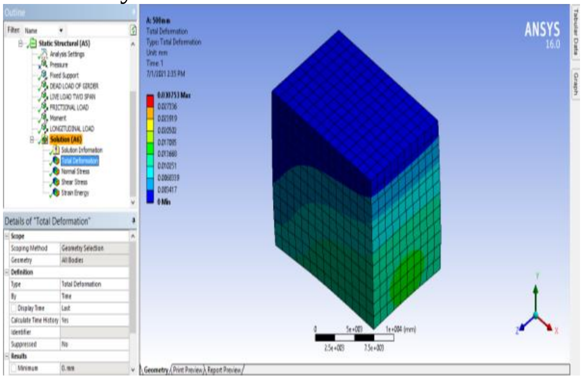

A: 500mm
Total Deformation
Type: Total Deformation
Unit: mm
Time: 1
7/1/2021 2:35 PM

0.030753 Max
0.027336
0.023919
0.020502
0.017085
0.013668
0.010251
0.0068339
0.003417
0 Min

Details of "Total Deformation"

Scope	
Scoping Method	Geometry Selection
Geometry	All Bodies
Definition	
Type	Total Deformation
By	Time
☐ Display Time	Last
Calculate Time History	Yes
Identifier	
Suppressed	No
Results	
☐ Minimum	0. mm

Fig 18: Total Deformation for Thickness 500mm

Above figure shows Total Deformation for thickness 500 mm in software ANSYS.

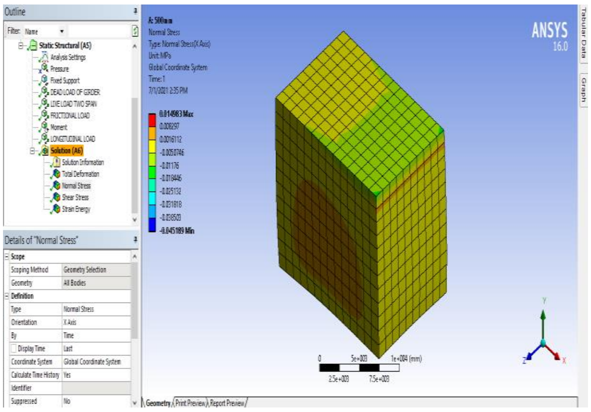

A: 500mm
Normal Stress
Type: Normal Stress(X Axis)
Unit: MPa
Global Coordinate System
Time: 1
7/1/2021 2:35 PM

0.014983 Max
0.008297
0.0016112
-0.0050746
-0.01176
-0.018446
-0.025132
-0.031818
-0.038503
-0.045189 Min

Details of "Normal Stress"

Scope	
Scoping Method	Geometry Selection
Geometry	All Bodies
Definition	
Type	Normal Stress
Orientation	X Axis
By	Time
☐ Display Time	Last
Coordinate System	Global Coordinate System
Calculate Time History	Yes
Identifier	
Suppressed	No

Fig 19: Normal stress for Thickness 500mm

Above figure shows Normal stress for thickness 500 mm in software ANSYS.

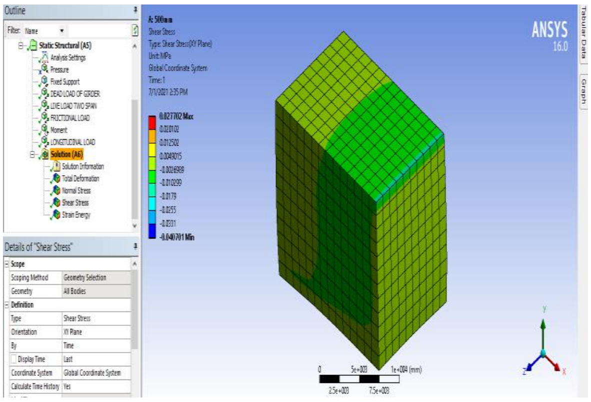

A: 500mm
Shear Stress
Type: Shear Stress(XY Plane)
Unit: MPa
Global Coordinate System
Time: 1
7/1/2021 2:35 PM

Details of "Shear Stress"

Scope
Scoping Method: Geometry Selection
Geometry: All Bodies
Definition
Type: Shear Stress
Orientation: XY Plane
By: Time
Display Time: Last
Coordinate System: Global Coordinate System
Calculate Time History: Yes

Fig 20: Shear Stress for Thickness 500mm

Above figure shows Shear stress for thickness 500 mm in software ANSYS.

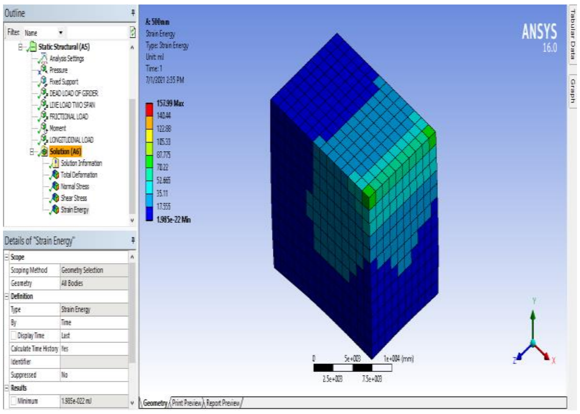

A: 500mm
Strain Energy
Type: Strain Energy
Unit: mJ
Time: 1
7/1/2021 2:35 PM

Details of "Strain Energy"

Scope
Scoping Method: Geometry Selection
Geometry: All Bodies
Definition
Type: Strain Energy
By: Time
Display Time: Last
Calculate Time History: Yes
Identifier:
Suppressed: No
Results
Minimum: 1.985e-022 mJ

Fig 21: Strain Energy for Thickness 500mm

Above figure shows Strain Energy for thickness 500 mm in software ANSYS.

4.7 Results for different diameters

Table 2: Total Deformation

TOTAL DEFORMATION mm	
ANALYTICAL	**ANSYS**
1.6	**1.76**

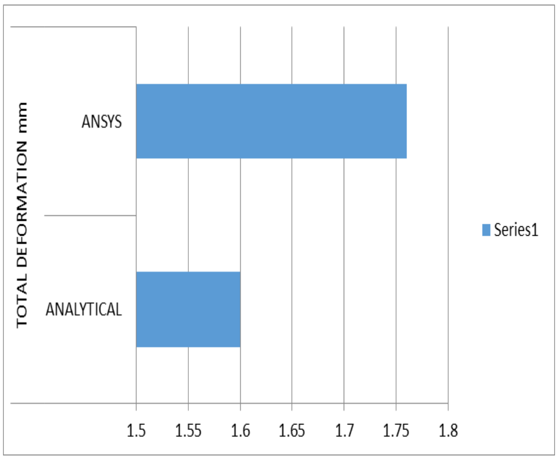

Graph.7.15 Total Deformation for diameter

Above graph describes the result total deformation, total deformation in Ansys results for diameter 1300mm is 1.76 mm and analytical result is 1.6 mm.

- **Normal Stress**

Table 1: Normal Stress for diameter

Normal Stress	
ANALYTICAL	**ANSYS**
4378.36815	**4816.204965**

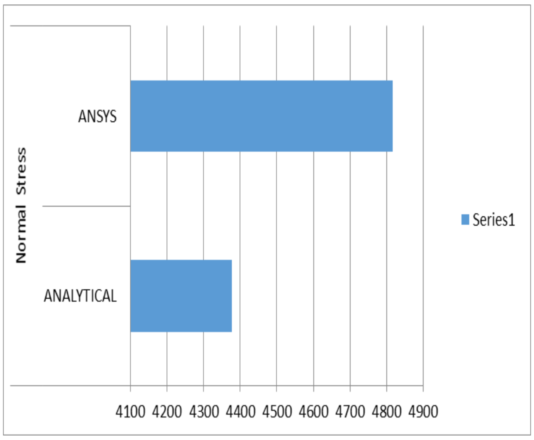

Graph: 22 Normal stress for diameter

Above graph describes the result total deformation, Normal Stress in Ansys results for diameter 1300mm is 1.4983e-002 MPa and analytical result is 4378.36815 MPa.

- **Shear Stress**

Table 3: Shear Stress for diameter

Shear stress	
ANALYTICAL	**ANSYS**
6.55242E-07	**7.20766E-07**

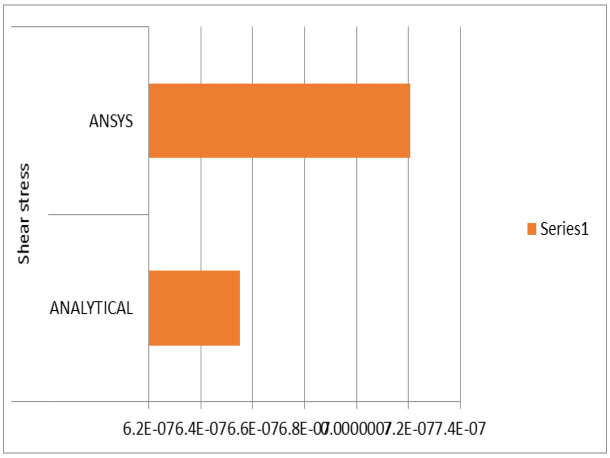

Graph 23: Shear stress for diameter

Above graph describes the result total deformation, Normal Stress in Ansys results for diameter 1300mm is 6.55242E-07 MPa and analytical result is 7.20766E-07 MPa.

- **Equivalent Stress**

Table 4: Equivalent Stress for diameter

Equivalent Stress	
ANALYTICAL	**ANSYS**
1.45833E-06	**1.60417E-06**

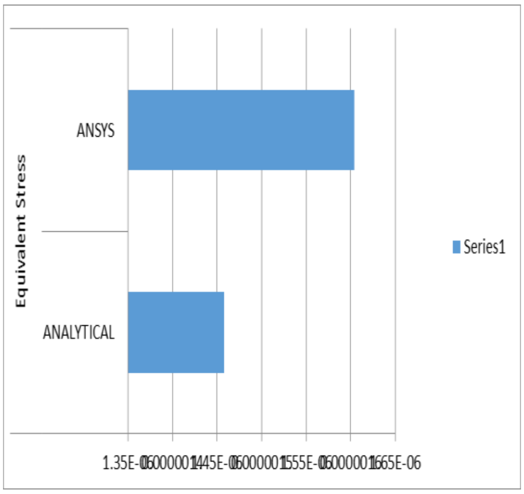

Graph 24: Equivalent Stress for diameter

Above graph describes the result total deformation, Equivalent Stress for diameter in Ansys results for diameter 1300mm is 1.45833E-06 MPa and analytical result is 1.60417E-06 MPa.

5. Conclusion:

- Piles' maximum settlement, settlement agreement, and load bearing capabilities are all substantially impacted by pile spacing under dynamic loading. The first stage of the literature study determines that the gap between the piles is well within the permitted range, which is also affected by the pressure conditions.
- The pile spacing must be lowered if the load works in the center of both mat constructions. Increased pile density minimizes total and ultimate settling while improving load bearing capacity up to a certain limit dictated by the loading scenario. Later in the process, the piling cap and foundations are modeled in ANSYS with references to the Krishna Bridge, and soil instability causes distortion of 96mm.
- All IS 11841 code requirements for NDCT design are studied in the initial stage of study, and a numerical model in ANSYS is proposed against identity and applied loads against various dimensions. Following an analysis, the following conclusions may be reached.
- The total deformations, normal stress, shear stress, and equivalent stress are explored with diverse soil conditions and soil types in this research impact of cyclic lateral load using time history analysis. The time history data used is Electro, which includes high, medium, and low amplitude.
- The soil types evaluated are soft, medium, and hard as defined by IS 1893-2016 and represented in ANSYS.
- It is possible to deduce that for silty and clay soil layers. Total deformation, normal stress, shear stress, and equivalent stress all decreased by 25-30%.
- If sandy soil or Type-I is found on the job site, extensive excavation or soil treatment is advised.
- Pile Foundation Results Using Different Diameters and Thicknesses:
- The results obtained by employing various diameters are 1300mm, 1400mm, and 1500mm. while the results obtained by employing various thicknesses are 300mm, 400mm, and

500mm.

- Results for various diameters:
- Overall deformation graph illustrates the total deformation result, total deformation for diameter 1300mm is 0.0308, total deformation for diameter 1400 is 0.0331, and total deformation for diameter 1500 is 0.0332. The results are listed in ascending order of diameter.
- The strain energy graph explains the outcome. Strain Energy is 157.99 for a diameter of 1300mm, 160.78 for a diameter of 1400mm, and 162.72 for a diameter of 1500mm. The results are listed in ascending order of diameter.
- A shear stress graph depicts the outcome. Shear stress is 0.0277 for a diameter of 1300mm, 0.0286 for a diameter of 1400mm, and 0.0315 for a diameter of 1500mm. The results are listed in ascending order of diameter.
- The outcome is described by a normal stress graph. Normal stress is 0.0150 for a diameter of 1300mm, 0.0144 for a diameter of 1400mm, and 0.0288 for a diameter of 1500mm. The results are listed in ascending order of diameter.

Results for different thickness:

- Entire deformation graph illustrates the total deformation result; total deformation for thickness 300mm is 0.0328, thickness 400mm is 0.0320, and thickness 500mm is 0.0308. The results are listed in decreasing order of thickness.
- The strain energy graph depicts the result strain energy, which is 162.28 for thickness 300mm, 160.49 for thickness 400mm, and 157.99 for thickness 500mm. The results are listed in decreasing order of thickness.
- A shear stress graph depicts the outcome. Shear stress is 0.0216 for thickness 300mm, 0.0244 for thickness 400mm, and 0.0277 for thickness 500mm. The result is in increasing order of thickness.
- The normal stress graph depicts the result normal stress, which is 0.0094 for thickness 300mm, 0.0124 for thickness 400mm, and 0.0150 for thickness 500mm. The result is in increasing order of thickness.
- The graph above shows the overall deformation result; total deformation for thickness 300mm is 0.0328, thickness 400mm is 0.0320, and thickness 500mm is 0.0308. The results are listed in decreasing order of thickness.

References:

1. Brungraber, R.J. and Kim, J.B. (1976). “Full-scale lateral load tests of pile groups.” Journal of Geotechnical Engineering. ASCE, Vol.102, No. GT1, pp. 87-105.
2. Meimon, Y., Baguelin, F. and Jezequel, J.F. (1986). “Pile group behavior under long term lateral monotonic and cyclic loading.” Proc., Third Int’l Conf. on Numerical Methods in Offshore Piling, Inst. Francais Du Petrole, Nantes, p. 286-302
3. Brown, D.A., Resse, L.C., and O’Neill, M.W. (1987). “Cyclic lateral loading of a large-scale pile group.” Journal of Geotechnical Engineering. ASCE, Vol.113, No. 11, pp.1326-1343.
4. Rollins, K. M., Peterson, K. T., and Weaver, T. J. (1998). “Lateral load behavior of full-scale pile group in clay.” J. of Geotechnical and Geoenvironmental Engineering, ASCE, Vol. 124, No.6, p. 468–478.
5. Dunnavant, T.W. and O’Neill, M.W. (1986). “Methodology for analysis of laterally loaded pile groups,” Third Intl. Conf. on Numerical Methods in Offshore Piling, IFDP/LCPC, Nantes, France, p. 303-316.
6. S. K. Haigh et. al “The response of pile groups under cyclic lateral loads”
7. Karsan R. Hirani at. el. “Lateral load carrying capacity of model pile groups.” National Conference on Recent Trends in Engineering & Technology
8. TouréYoussoufat. el. “Force Performance Analysis of Pile Behavior of the Lateral Load” MPDI 28 March 2019